Journal of Alloys and Compounds 480 (2009) 107–110

Contents lists available at ScienceDirect

Journal of Alloys and Compounds

journal homepage: www.elsevier.com/locate/jallcom

Synthesis and structural characterization of twinned V-shaped IrO_2 nanowedges on TiO_2 nanorods via MOCVD

C.A. Chen[a], Y.M. Chen[a], Y.S. Huang[a,*], D.S. Tsai[b], P.C. Liao[c], K.K. Tiong[d]

[a] Department of Electronic Engineering, National Taiwan University of Science and Technology, Taipei 106, Taiwan
[b] Department of Chemical Engineering, National Taiwan University of Science and Technology, Taipei 106, Taiwan
[c] Department of Electronic Engineering, Technology and Science Institute of Northern Taiwan, Taipei 112, Taiwan
[d] Department of Electrical Engineering, National Taiwan Ocean University, Keelung 202, Taiwan

ARTICLE INFO

Article history:
Received 26 June 2008
Received in revised form
16 September 2008
Accepted 16 September 2008
Available online 20 November 2008

PACS:
81.07.Bc
81.15.Gh
61.05.C–
61.46.–w

Keywords:
TiO_2 and IrO_2
Metal organic chemical vapor deposition
X-ray diffraction
Scanning electron microscopy
Transmission electron microscopy

ABSTRACT

IrO_2 nanocrystals (NCs) were grown on top of rutile (R) TiO_2 nanorods (NRs) sitting on sapphire (SA) (1 0 0) substrate via metal organic chemical vapor deposition by using $(C_6H_7)(C_8H_{12})Ir$ and $Ti[OCH(CH_3)_2]_4$ as source reagents. The surface morphology and structural properties of the as-deposited NCs were characterized. The field-emission scanning electron microscopy images and X-ray diffraction patterns indicate growth of V-shaped IrO_2(1 0 1) nanowedges (NWs) on top of R-TiO_2 NRs. Transmission electron microscopy and selected-area electron diffractometry characterizations of IrO_2 NCs showed that the NWs were crystalline IrO_2 with a twin plane of (1 0 1) and twin direction of [$\bar{1}$ 0 1] at the V-junction.

1. Introduction

Fabrication of one-dimensional (1D) nano-scaled materials, such as nanotubes (NTs) and nanorods (NRs), has gained considerable attention owing to interests in fundamental science and the potential in developing nanodevices [1,2]. The development of nanodevices has benefitted from the distinct morphology, huge surface area and high aspect ratio of NTs and NRs. More recently, the technology has advanced to deposit various materials using 1D nanostructures as templates [3]. Such an approach not only provides a convenient way to grow 1D nanostructures from materials that are difficult to be fabricated into 1D form by themselves, but also paves the way to synthesize 1D heteronanostructures. The obtained 1D heteronanostructure from this approach has been shown to demonstrate enhanced functionality [4,5].

Recently, we have successfully grown well-aligned rutile (R) phase TiO_2 NRs [6] and nanostructural IrO_2 [7] on sapphire substrate via metal organic chemical vapor deposition (MOCVD). Nanostructural TiO_2 has been widely studied as a very promising material for applications in photocatalysis [8], sensors [9], solar energy conversion [10] and optical devices [11]. IrO_2 is a good electric conductor with high thermal and chemical stability, and depositing IrO_2 nanocrystals on TiO_2 NRs to form 1D heteronanostructures may be useful in electrical and electrochemical applications. The IrO_2 has the lattice constant close to that of R-TiO_2 (IrO_2: $a = b = 0.450$ nm and $c = 0.316$ nm [JCPDS no. 15-0870]; TiO_2: $a = b = 0.459$ nm and $c = 0.296$ nm [JCPDS no. 21-1276]). Owing to the proximate lattice constant and identical crystal structure, a heteroepitaxial growth of IrO_2 on R-TiO_2 NRs may be readily facilitated [12].

In this work, we report the growth of V-shaped IrO_2 nanowedges (NWs) on top of R-TiO_2 NRs via MOCVD. The source reagents were $(C_6H_7)(C_8H_{12})Ir$ and titanium (IV) i-propoxide ($Ti[OCH(CH_3)_2]_4$ (TTIP)). The surface morphology and structural properties of the as-deposited NCs were characterized by field-emission scanning

* Corresponding author. Tel.: +886 2 27376385; fax: +886 2 27376424.
E-mail address: ysh@mail.ntust.edu.tw (Y.S. Huang).

0925-8388/$ – see front matter © 2008 Elsevier B.V. All rights reserved.
doi:10.1016/j.jallcom.2008.09.173

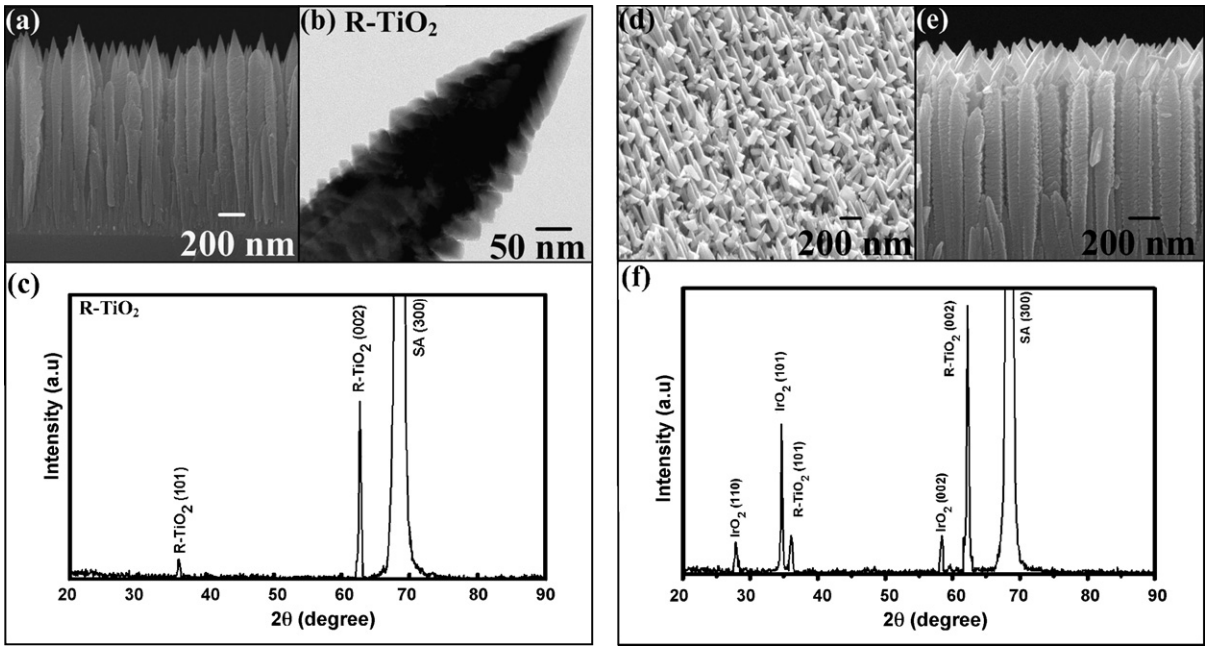

Fig. 1. (a) FESEM images of R-TiO_2 NRs, (b) the cross-sectional TEM image of a single R-TiO_2 NR, and (c) the XRD pattern of TiO_2 NRs deposited on SA(1 0 0). FESEM images of IrO_2 NCs deposited on top of R-TiO_2 NRs: (d) 30° perspective view and (e) cross-sectional view images. (f) The XRD pattern of IrO_2 NCs grown on top of TiO_2 NRs sitting on the SA(1 0 0) substrate.

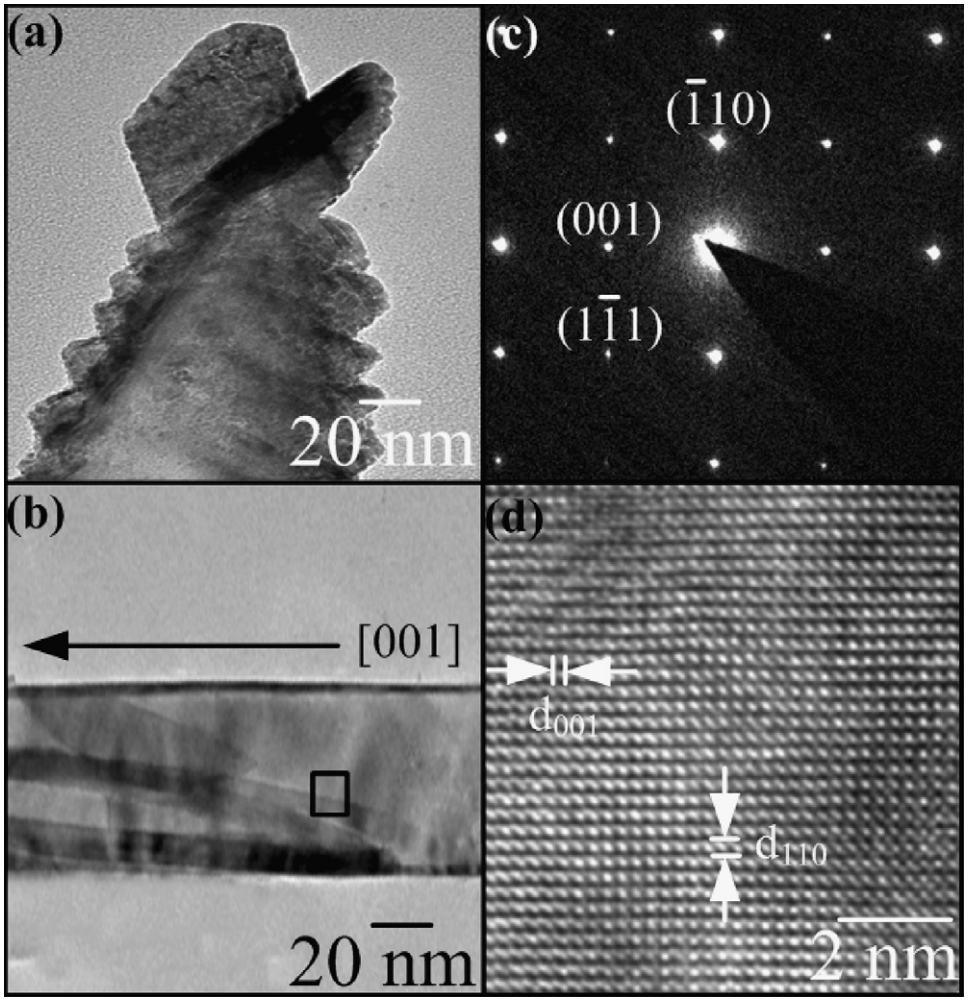

Fig. 2. (a) The cross-sectional TEM image of a single V-shaped IrO_2 NW on top of R-TiO_2 NR, (b) the cross-sectional TEM image along zone axis [1 1 0] focused on one arm of the V-shaped IrO_2 NW, (c) the SAED pattern projection along [1 1 0] zone axis, and (d) high-resolution TEM taken from the wedge sidewall marked in (b).

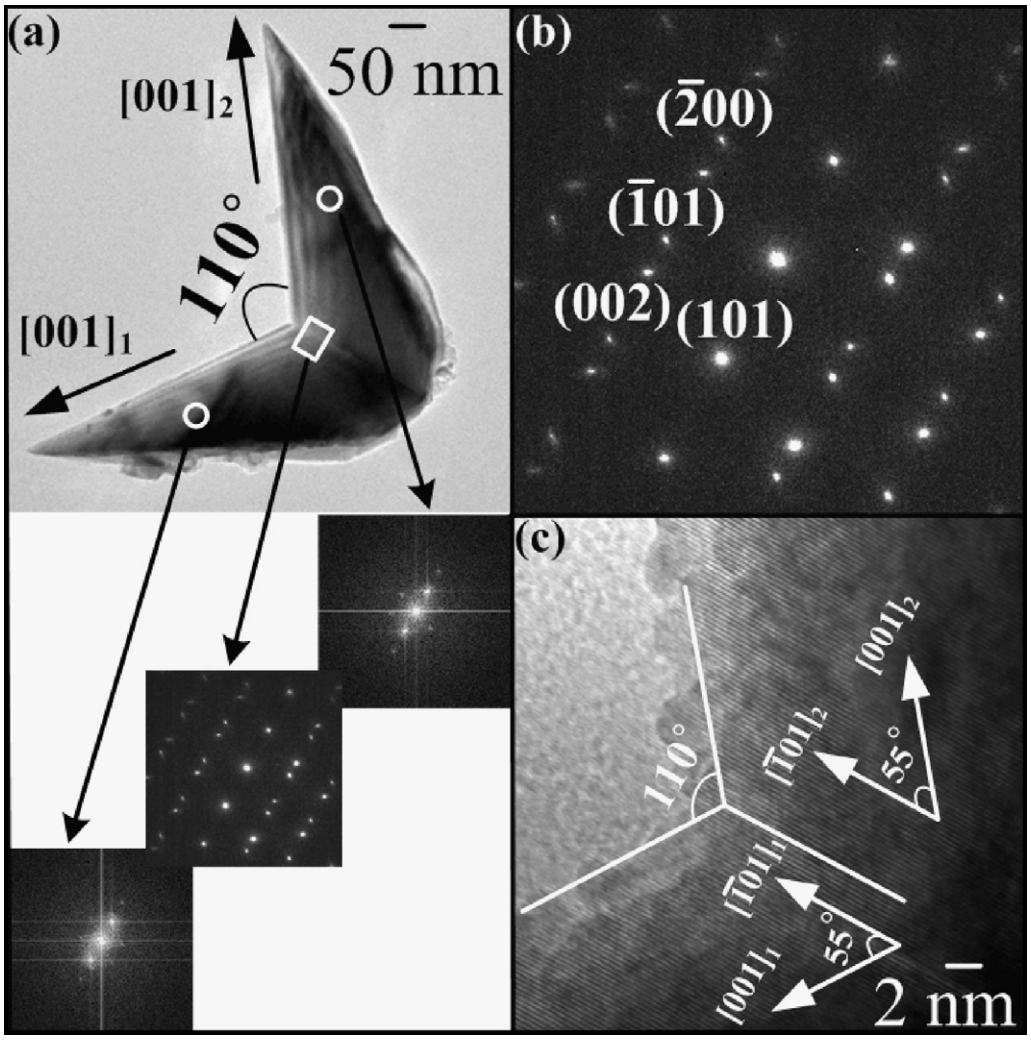

Fig. 3. (a) The TEM image of a free standing V-shaped IrO_2 NW with SAED patterns, showing the junction and the arms (b) the SAED pattern along the [0 1 0] zone axis of the junction and (c) the HRTEM images in the vicinity of the V-shaped junction regime.

electron microscopy (FESEM), X-ray diffraction (XRD), transmission electron microscopy (TEM) and selected-area electron diffractometry (SAED). The formation of V-shaped IrO_2 NWs with a twin structure at the V-junction sitting on top of R-TiO_2 NRs is presented.

2. Experimental

The growth of IrO_2 NWs on TiO_2 NRs was carried out in a vertical-flow cold wall MOCVD system, using $(C_6H_7)(C_8H_{12})$Ir and TTIP as source reagents. The substrate was sapphire (SA) (1 0 0). The details for TiO_2 NRs and IrO_2 nanocrystals growth were described in Refs. [6] and [7], respectively.

A JEOL-JSM6500F FESEM was used to study the morphology of IrO_2 NWs grown on R-TiO_2 NRs. The growth orientations were examined using a Rigaku D/Max-RC X-ray diffractometer (XRD) equipped with Cu Kα radiation source and Ni filter at a wavelength of 1.5418 Å. TEM images and SAED patterns were recorded to characterize the structure of the individual V-shaped IrO_2 NC by a Phillips Tecnai G2 F20 FE-TEM at working voltage of 200 kV.

3. Results and discussion

As illustrated in Fig. 1(a), the FESEM images show densely packed vertically aligned TiO_2 NRs with sharp tips grown on SA(1 0 0) substrate. The TEM image of a single TiO_2 NR shown in Fig. 1(b) indicating the striation growth along *c* axis. Fig. 1(c) shows the XRD pattern of TiO_2 NRs deposited on the SA(1 0 0), where the main reflection peaks are identified to be from the R-TiO_2 (0 0 2) and SA (3 0 0), indicating pure rutile phase with a (0 0 1) preferred orientation has been deposited. Fig. 1(c) also indicates the presence of a weak R-TiO_2 (1 0 1) feature located around 36°. The FESEM images and XRD pattern of the TiO_2 NRs grown on SA(1 0 0) reveal the uniquely single-directional growth of rutile phase TiO_2 NRs along [0 0 1] with (1 0 1) planes on the tips of NRs. The R-TiO_2 NRs were then used as template for IrO_2 NCs deposition. FESEM micrographs depicted in Fig. 1(d) and (e) respectively, display 30° perspective view and cross-sectional view images of IrO_2 NCs deposited on top of TiO_2 NRs. As can be seen in Fig. 1(d) and (e), the well-aligned V-shaped IrO_2 with two wedge-like arms were grown on top of R-TiO_2 NRs. Fig. 1(f) displays the XRD pattern of IrO_2 NCs grown on top of TiO_2 NRs. The XRD pattern indicates a preferred orientation of IrO_2 (1 0 1) NCs has been deposited.

Further structural characterization of the IrO_2 NWs on R-TiO_2 NRs was performed using TEM. Fig. 2(a) displays the TEM image of a single V-shaped IrO_2 wedge-like nanocrystal on top of R-TiO_2 nanorod. Fig. 2(b) shows the TEM image focused on one arm of the V-shaped IrO_2 NW. Fig. 2(c) is the SAED pattern taken from the wedge sidewall. The SAED pattern has been identified to be the [1 1 0] zone pattern, indicating that the wedge walls belong to the {1 1 0} facets and the preferential growth direction of the IrO_2 wedge is along the [0 0 1] direction (*c*-axis). Fig. 2(d) displays

the high-resolution TEM image taken from the wedge marked in Fig. 2(b) exhibiting the clear lattice plane of the IrO_2 wedge. The lattice spacing between adjacent lattice planes for the (0 0 1) and (1 1 0) planes are 0.322 nm and 0.325 nm, respectively. The results also confirmed the tetragonal rutile structure and single-crystalline quality of the IrO_2 NCs.

Fig. 3(a) shows the TEM image of a free standing V-shaped IrO_2 nanocrystal with two wedge-like arms. The SAED pattern along the [0 1 0] zone axis of the junction depicted in Fig. 3(b) shows an overlap of two series of doublet spots, a result of intersecting two arms of different orientations. The HRTEM images were processed by fast Fourier transform (FFT) to examine the V-shaped junction of IrO_2 NWs in detail. Fig. 3(c) shows the HRTEM images in the vicinity of the V-shaped junction regime with the orientation relationship of major axes [0 0 1] and $[\bar{1}\,0\,1]$. It is clear that the preferential growth direction for the wedges is the [0 0 1] direction. From a detailed analysis of Fig. 3(b) and (c), it can be concluded that the V-shaped NWs have a single twin structure at the junction. The twin plane is (1 0 1) and the twin direction is $[\bar{1}\,0\,1]$. The twin boundary is coherent and the two near symmetric arms are separated by an angle of $\sim 110^\circ$.

4. Summary

IrO_2 NCs were grown on top of the tips of R-TiO_2 NRs deposited on SA(1 0 0) substrate. FESEM micrographs and XRD patterns revealed the bifurcated growth of twinned V-shaped IrO_2 (1 0 1) with two wedge-like arms sitting on top of R-TiO_2 NRs. TEM, SAED and HRTEM characterizations of the NWs confirmed that the wedges were crystalline IrO_2 with a single twin structure with (1 0 1) twin plane along $[\bar{1}\,0\,1]$ twin direction.

Acknowledgements

The authors acknowledge the support of the National Science Council of Taiwan under Contract Nos. NSC 96-2112-M-011-001 and NSC 97-2112-M-011-001-MY3.

References

[1] Y. Xia, P. Yang, Y. Sun, Y. Wu, B. Mayers, B. Gates, Y. Yin, F. Kim, H. Yan, Adv. Mater. 15 (2003) 353–389.
[2] C.S. Lao, P.X. Gao, L. Zhang, D. Davidovic, R. Tummala, Z.L. Wang, Nano Lett. 6 (2006) 263–266.
[3] S.O. Obare, N.R. Jana, C.J. Murphy, Nano Lett. 1 (2001) 601–603.
[4] S. Han, C. Li, Z. Liu, B. Lei, D. Zhang, W. Jin, X. Liu, T. Tang, C. Zhou, Nano Lett. 4 (2004) 1241–1246.
[5] D. Zhang, Z. Liu, S. Han, C. Li, B. Lei, M.P. Stewart, J.M. Tour, C. Zhow, Nano Lett. 4 (2004) 2151–2155.
[6] C.A. Chen, Y.M. Chen, A. Korotcov, Y.S. Huang, D.S. Tsai, K.K. Tiong, Nanotechnology 19 (2008) 75611-1–075611-5.
[7] R.S. Chen, A. Korotcov, Y.S. Huang, D.S. Tsai, Nanotechnology 17 (2006) R67–R87.
[8] S.P. Albu, A. Ghicov, J.M. Macak, R. Hahn, P. Schmuki, Nano Lett. 7 (2007) 1286–1289.
[9] C. Garzekka, E. Comini, E. Tempestis, C. Frugeru, G. Sberveglieri, Sens. Actuators B 68 (2000) 189–196.
[10] B. O'Regan, M. Gratzel, Nature 353 (1991) 737–740.
[11] A. Richel, N.P. Johnson, D.W. McComb, Appl. Phys. Lett. 76 (2002) 1816–1818.
[12] T. Akita, M. Okumura, K. Tanaka, S. Tsubota, M. Haruta, J. Electron Microsc. 52 (2003) 119–124.